0026-895X/98/050902-06$3.00/0

MOLECULAR PHARMACOLOGY, **53:**902–907 (1998).

Isoform-Specific Inhibition of L-Type Calcium Channels by Dihydropyridines Is Independent of Isoform-Specific Gating Properties

HAI HU AND EDUARDO MARBAN

Section of Molecular and Cellular Cardiology, Department of Medicine, The Johns Hopkins University School of Medicine, Baltimore, Maryland 21205

Received December 8, 1997; Accepted February 4, 1998

This paper is available online at http://www.molpharm.org

ABSTRACT

Dihydropyridines (DHPs) block L-type Ca^{2+} channels more potently at depolarized membrane potentials, consistent with high affinity binding to the inactivated state. Nisoldipine (a DHP antagonist) blocks the smooth muscle channel more potently than the cardiac one, a phenomenon observed not only in native channels but also in expressed channels. We examined whether this tissue specificity was attributable to differences of inactivation in the two channel types. We expressed cardiac or smooth muscle α1C subunits in combination with β2a and α2/δ subunits in human embryonic kidney cells, and used 2 mM Ca^{2+} as the permeant ion. This system thus reproduces the *in vivo* topology and charge carrier of the channels while facilitating comparison of the two α1C splice variants. Both voltage-dependent and isoform-specific sensitivity of 10 nM nisoldipine inhibition of the channel were demonstrated, with the use of −100 mV as the holding potential for fully reprimed channels and −65 mV to populate the inactivated state. Under drug-free conditions, we characterized fast inactivation (1-sec prepulses) and slow inactivation (3 min prepulses) in the two isoforms. Inactivation parameters were not statistically different in the two channel isoforms; if anything, cardiac channels tended to inactivate more than the smooth muscle channels at relevant voltages. Likewise, the voltage-dependent activation was identical in the two isoforms. We thus conclude that the more potent nisoldipine inhibition of smooth muscle versus cardiac L-type Ca^{2+} channels is not attributable to differences in channel inactivation or activation. Intrinsic, gating-independent DHP receptor binding affinity differences must be invoked to explain the isoform-specific sensitivity of the DHP block.

In cardiovascular cells, DHPs block L-type Ca^{2+} channels more potently at depolarized membrane potentials (Bean, 1984; Hess *et al.,* 1984; Sanguinetti and Kass, 1984; Schwartz *et al.,* 1984). This observation has been interpreted as evidence that DHPs bind with high affinity to the inactivated state of the channels (Bean, 1984; Sanguinetti and Kass, 1984). If so, DHPs would interact with Ca^{2+} channels in a manner analogous to the interaction between local anesthetics and Na^{+} channels (Hille, 1977). DHPs function more potently on SM than on cardiac muscle or neurons (Triggle, 1991); indeed, such specificity has been suggested to reflect voltage-dependent inhibition because, in general, the resting membrane potential of SM cells is more positive than that of myocardial cells (Nelson *et al.,* 1988; Triggle, 1991).

The cloning and functional expression of Ca^{2+} channels have made it possible to study isoform-specific pharmacological properties in well controlled systems. L-type Ca^{2+} channels are composed of three to four subunits; the pore-forming α1 is the primary subunit and the rest (α2/δ, β, and/or γ) are auxiliary subunits (Perez-Reyes and Schneider, 1995; Catterall, 1996). Cardiac and SM channels share β subunit isoforms (β2a) and seem not to express the γ subunit (Perez-Reyes and Schneider, 1995). The α1 subunit is the target of many drugs, including DHPs (Vaghy *et al.,* 1987; Triggle *et al.,* 1989). The α1C-a (Mikami *et al.,* 1989) and the α1C-b (Biel *et al.,* 1990) isoforms are alternatively spliced from the same α1C gene, with 95% similarity. The 5% differences are located at four sites, which are in the amino terminus, the transmembrane segments IS6 and IVS3, and an insert in the linker connecting domains I and II for α1C-b. Studies of cloned Ca^{2+} channels expressed in mammalian cells indicate that α1C subunits alone are sufficient to produce the tissue-specific DHP sensitivity difference (Welling *et al.,* 1993, 1997). Specifically, with α1C-a or α1C-b alone in Chinese

This work was supported by National Institutes of Health Grants R01-HL52768 (E.M.) and T32-HL07227 (H.H.).

ABBREVIATIONS: DHP, dihydropyridine; α1C-a, the α1 subunit of the cardiac L-type Ca^{2+} channel; α1C-b, the α1 subunit of the smooth muscle L-type Ca^{2+} channel; ANCOVA, analysis of covariance; EGTA, ethylene glycol bis(β-aminoethyl ether)-*N*,*N*,*N*′,*N*′-tetraacetic acid; HEK, human embryonic kidney; HEPES, 4-(2-hydroxyethyl)-1-piperazineethanesulfonic acid; I_{Ca}, peak Ca^{2+} current through the L-type Ca^{2+} channels; SM, smooth muscle; V_h, membrane holding potential.

hamster ovarian cells and 30 mM Ba^{2+} as the charge carrier, nisoldipine blocked both isoforms of the channel more potently at −40 mV holding potential than at −80 mV, with a higher affinity for the α1C-b channels. Recently, Welling and colleagues (1997) reproduced these findings in the HEK 293 expression system, using α1C subunits truncated at the carboxyl-terminal. They further identified the IS6 segment of the α1C subunit as the agent responsible for the tissue specificity of nisoldipine inhibition.

Both voltage-dependent and tissue-specific nisoldipine inhibition of Ca^{2+} currents in native channels and Ba^{2+} currents in expressed channels has been reported. Nevertheless, there is no direct evidence linking or separating the tissue specificity from possible isoform-specific differences in gating. To investigate the links between isoform-specific gating and drug block, we expressed α1C-a or α1C-b + β2a + α2/δ channels in HEK 293 cells, and used 2 mM Ca^{2+} as the charge carrier to achieve more physiologically relevant conditions. This system is thus close to the *in vivo* topology of the channels, yet contrasting the two α1C splice variants is much easier than in native cells.

We are interested in elucidating (1) whether voltage-dependent and isoform-specific DHP inhibition can be reproduced in our expression system and (2), more importantly, whether the isoform specificity is due to differences in gating.

Materials and Methods

Functional expression of cardiac and smooth muscle Ca^{2+} channel α1C subunits. The transient transfection of L-type Ca^{2+} channels in HEK 293 cells was performed as described previously (Hu *et al.,* 1997). Briefly, HEK 293 cells were maintained in Dulbecco's modified Eagle's medium with glucose and L-glutamine, supplemented with 10% fetal calf serum (GIBCO-BRL, Gaithersburg, MD) and 1% penicillin and streptomycin (GIBCO-BRL). Cells were plated on 35-mm Petri dishes at a density of 0.2 million cells/dish 1 day before transfection, and maintained in a 37° incubator. Cells were then transfected by calcium phosphate precipitation (Graham and van der Eb, 1973; Calcium Phosphate Transfection System, GIBCO-BRL) with 2–3 μg/dish plasmid DNA encoding Ca^{2+} channel subunits (see below), 0.5 μg/dish simian virus 40 T-antigen, and 0.2 μg/dish mitochondrially targeted green fluorescent protein (Marshall *et al.,* 1995). The calcium phosphate-DNA mixture was left on cells for 5–6 hr before being washed with phosphate-buffered saline and the addition of fresh media. The admixture of green fluorescent protein cDNA enabled us to identify transfected cells visually by fluorescent excitation (Marshall *et al.,* 1995).

Cells were transfected with plasmid DNA encoding the rabbit cardiac L-type Ca^{2+} channel α1 subunit $\alpha_{1C\text{-}a}$ (Mikami *et al.,* 1989) or the SM α1 subunit α1C-b (Biel *et al.,* 1990), in combination with equimolar quantities of rat cardiac β2a subunit (Perez-Reyes *et al.,* 1992) and rabbit skeletal muscle α2/δ subunit DNA (Ellis *et al.,* 1988).

Electrophysiology and data processing. Electrophysiological recordings were made 18–72 hr after transfection. Membrane current was recorded using the whole-cell patch configuration (Hamill *et al.,* 1981), with bath solution containing 2 mM $CaCl_2$, 147 mM CsCl, and 10 mM HEPES (titrated to pH 7.4 with CsOH). Pipettes were pulled from borosilicate glass and fire-polished to resistance of 0.5–2 MΩ when filled with pipette solution containing 108 mM CsCl, 4.5 mM MgATP, 9 mM EGTA, and 9 mM HEPES (titrated to pH 7.4 with CsOH). In the whole-cell configuration, the series resistance was typically 2–5 MΩ. In most of the experiments the series resistance was not compensated; this would have introduced a maximal voltage error of < 2.5 mV as the peak current magnitude was generally < 500 pA.

A coverslip with cells was placed in a 0.3 ml perfusion chamber connected to a gravity-driven perfusion system. Flow was maintained throughout the experiment at rates of 0.5–2 ml/min. Whole-cell currents were measured >10 min after patch rupture to allow for equilibration between intracellular and pipette solutions. Currents were elicited by 10–25-msec depolarizing pulses to 0 mV from a given holding potential (−100, −80, or −65 mV, as indicated). When current-voltage relationships were measured, the cell was depolarized to a family of potentials (−50 to +60 mV) for 25 msec from V_h = −80 mV, at intervals of 20 sec. When the inactivation curves were measured, sufficient time (20 sec for fast inactivation and ≥5 min for slow inactivation) at V_h = −80 mV was allowed for channels to recover from inactivation between pulses. Currents were recorded using a patch-clamp amplifier (Axopatch 200; Axon Instruments, Foster City, CA), and sampled at 10 kHz after analog filtering at 2–5 kHz. To quantify ionic current amplitude, data were leak-subtracted by a P/4 protocol. Acquisition and analysis of the data were performed with custom software.

A stock solution of 10 mM nisoldipine was prepared by dissolving nisoldipine powder (kindly supplied by Bayer, Wuppertal, Germany) in polyethylene glycol 400 (Sigma, St. Louis, MO); it was then stored in the dark at −80°. The nisoldipine solutions at the final concentrations were freshly prepared before experiments and protected from light. All experiments were conducted at room temperature of 21–22° and all those involving nisoldipine were conducted in the dark.

Statistics. Pooled data are presented as mean ± standard error. Statistical comparison was evaluated by the two-tailed paired or unpaired Student's *t* test, or ANCOVA, where appropriate, with $p < 0.05$ considered significant.

Results

We first confirmed and characterized the voltage dependence of nisoldipine inhibition on Ca^{2+} channels in our expression system. Fig. 1A shows the effect of 10 nM nisoldipine on I_{Ca} through α1C-a + β2a + α2/δ channels, which is the cardiac isoform. In Fig. 1, the *top* shows representative currents recorded at the times indicated at the *bottom*. The voltage protocol used is illustrated on top of record a. Fig 1A, *bottom*, plots the time course of peak I_{Ca}. The cell was first held at −100 mV, a V_h at which the channels were fully reprimed (trace a). Then the V_h was changed to −65 mV (□); slow inactivation was observed, stabilizing in 3–4 min, with a relative remaining current of 49% (trace b). Introduction of 10 nM nisoldipine potently blocked the current at V_h = −65 mV (7% remaining, trace c), yet when the cell was repolarized to V_h = −100 mV, an unblocking effect was observed, and I_{Ca} recovered to 48% of the original amplitude, despite the fact that 10 nM nisoldipine was still present (trace d). Note that polyethylene glycol 400 itself, as the solvent for nisoldipine, has no effect on I_{Ca} even at concentrations 1000 times higher than those used in the present study (Kass and Scheuer, 1982).

Despite the differences in the absolute V_h values chosen here compared with those in previous studies (Welling *et al.* 1993, 1997), these findings are entirely consistent with earlier studies after correction for surface charge effects on the cell membrane potential. Recall that previous studies, which used −80 and −40 mV holding potentials, were performed with 30 mM Ba^{2+} as the charge carrier, which would be expected to cause an ~20 mV depolarizing voltage shift (Kass and Krafte, 1987; McDonald *et al.,* 1994).

Using the same protocol, we examined the effect of nisoldipine on I_{Ca} through the SM channel (α1C-b + β2a + α2/δ). Fig. 1B shows a representative experiment. Three differences

were observed when these results were compared with those of the cardiac channels. First, the SM channel inactivated less at $V_h = -65$ mV; second, 10 nM nisoldipine blocked the SM channels more completely than the cardiac channels; third, after the cell was repolarized to $V_h = -100$ mV, the unblocking effect was less prominent.

Fig. 2 summarizes the effects of nisoldipine inhibition on the two channel isoforms. For both, nisoldipine blocked more potently at −65 mV, when channels were partly inactivated, than at −100 mV when the channels were fully reprimed, in line with the idea of inactivated-state inhibition. Among the three differences between the two channel isoforms, the first (steady state inactivation at −65 mV) was not statistically significant, yet the probability of null hypothesis $p = 0.056$ indicates a strong trend that the cardiac channel inactivated more than the SM one at $V_h = -65$ mV. The second difference (inhibition at $V_h = -65$ mV) and the third (inhibition at $V_h = -100$ mV) were unambiguously significant, and they agree with previously published results (Welling *et al.,* 1993, 1997). The first difference, that in drug-free steady state inactivation, would thus not help to explain the second difference if the nisoldipine inhibition depended mainly on the inactivated state as suggested by studies in native cells (Bean, 1984; Sanguinetti and Kass, 1984): when channels are more inactivated, block by nisoldipine should be *more* potent, not less as observed here.

To extend these observations, we quantified the voltage dependence of inactivation of both types of channels under drug-free conditions. The results shown in Fig. 1 indicate that channels inactivate with two distinct time courses during changes of V_h from −100 to −65 mV. A fast component of inactivation, which appears within seconds, is followed by a slower component, which is complete only over ~3 min. We first measured the fast inactivation curves of the channels, using 1-sec prepulses from $V_h = -80$ mV; the results are shown in Fig. 3A, with the voltage protocol illustrated as an inset. For each channel type, 10 complete individual inactivation curves were obtained. The pooled data of inactivation

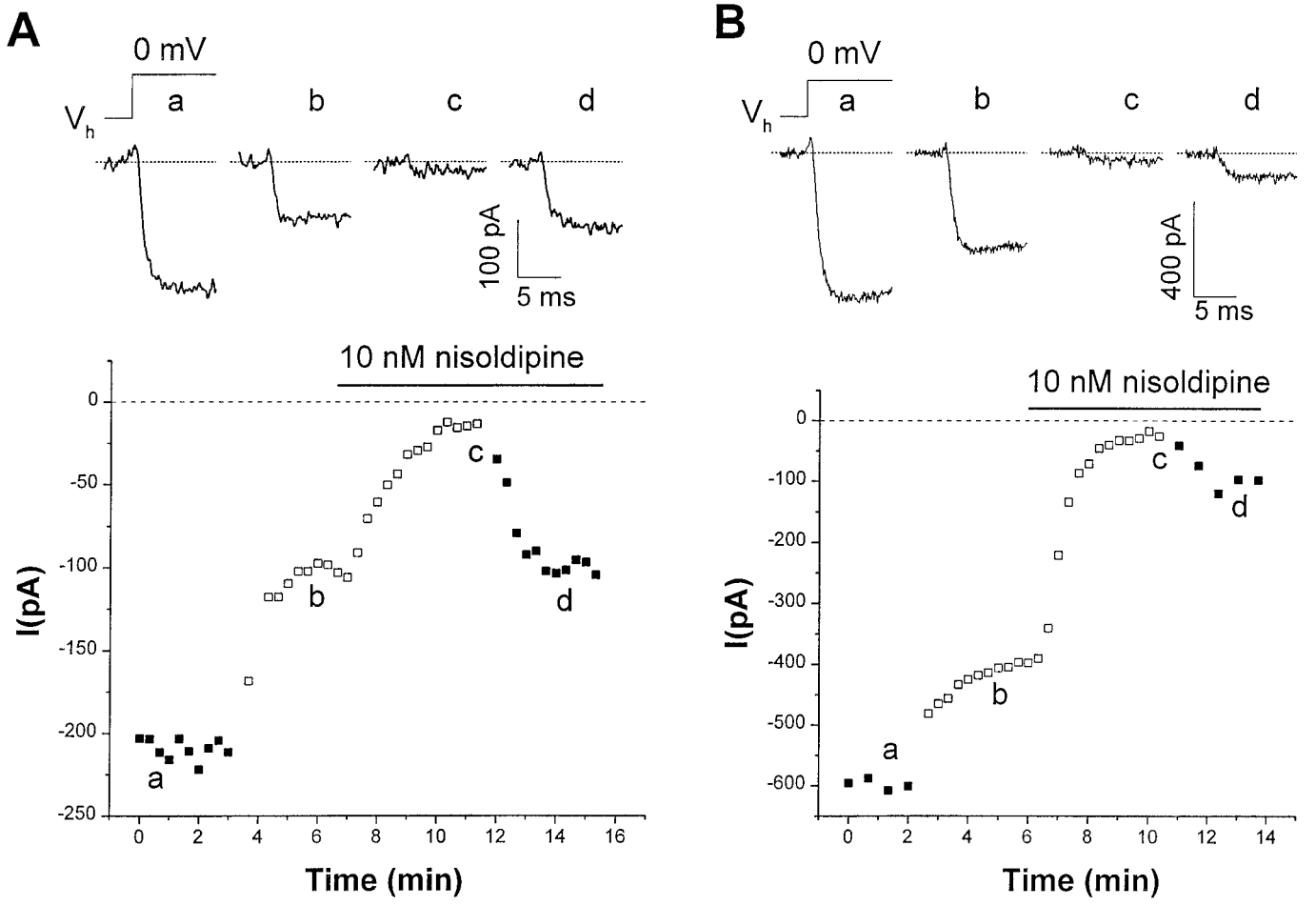

Fig. 1. A, Effects of nisoldipine and V_h on I_{Ca} from the cardiac channel α1C-a + β2a + α2/δ expressed in HEK 293 cells. *Top,* Representative currents from $V_h = -100$ mV (a, d) or −65 mV (b, c) at steady state, in the absence (*a*, *b*) or presence (*c*, *d*) of 10 nM nisoldipine, recorded at the times *a*, *b*, *c*, and *d* indicated in B. The voltage protocol is shown on top of *trace a*. The records shown were smoothed using a two-adjacent-point averaging method. *Bottom,* Time course of I_{Ca}. The cell was first held at −100 mV (■) and then −65 mV (□) in normal saline. After steady state inactivation was reached at −65 mV, 10 nM nisoldipine solution was applied and the current was dramatically suppressed. Still in the presence of nisoldipine, changing V_h back to −100 mV largely unblocked the current. B, Effects of nisoldipine and V_h on I_{Ca} from the SM channel α1C-b + β2a + α2/δ expressed in the HEK 293 cells. *Top,* Representative currents from $V_h = -100$ mV (*a*, *d*) or −65 mV (*b*, *c*) at steady state, in the absence (*a*, *b*) or presence (*c*, *d*) of 10 nM nisoldipine, recorded at the times *a*, *b*, *c*, and *d* indicated. The voltage protocol is shown above *trace a*. Unlike those in Fig. 1A, records plotted here are not smoothed. *Bottom,* Time course of I_{Ca}. The cell was first held at −100 mV (■) and then −65 mV (□) in normal saline. After steady state inactivation was reached at −65 mV, 10 nM nisoldipine solution was applied and the current was almost completely inhibited. Still, in the presence of nisoldipine, changing V_h back to −100 mV partly unblocked the current.

were normalized to enable the Boltzmann fits of the curves to reach unity, with an equation of $I_{relative} = A + (1-A)/[1 + \exp(V_p - V_{½})/k]$ where $I_{relative}$ is the relative remaining current, A is the fraction of the incomplete inactivation, V_p is the prepulse membrane potential, $V_{½}$ is the potential at which one-half of the channels are inactivated, and k is the slope. The fitting of the mean inactivation for the cardiac channels gave $V_{½} = -35$ mV, $k = 17$ mV, and $A = 0.32$, and for the SM channels, $V_{½} = -30$ mV, $k = 9$ mV, and $A = 0.29$. There is a trend that, at voltages more negative than −30 mV, the cardiac channels are more inactivated, but there were no significant differences in either $V_{½}$ or k in the two groups.

Because Fig. 1 shows that it takes several minutes to reach steady state inactivation, we considered not only fast inactivation but also the less well-characterized slow inactivation process. We therefore studied inactivation of the channels with 3 min prepulses. The corresponding recovery was slower when compared with that needed for fast inactivation, and we allowed ≥5 min for recovery at −80 mV between pulses. A brief test pulse (10 msec) to 0 mV was applied every 20 sec to monitor the recovery at −80 mV. The two steady state currents elicited from −80 mV on either side of each inactivation prepulse were averaged to obtain the reference current.

Fig. 3B shows the results of 3-min prepulse inactivation. Compared with Fig. 3A, the prolonged inactivation shifted the curves dramatically to the left, and the saturating inactivation reached 100% instead of 60–70% as in the fast inactivation. Data were collected from 12 cells expressing cardiac channels and 14 cells expressing SM channels; each point represents data from 3 to 6 cells. Boltzmann fitting of the mean values using $I_{relative} = [1 + \exp(V_p - V_{½})/k]^{-1}$ gave $V_{½} = -57$ mV and $k = 9$ mV for the cardiac channels, and $V_{½} = -49$ mV and $k = 10$ mV for the SM channels. ANCOVA, however, did not show a significant difference between the two original groups of data. There was a trend, however, for the cardiac curve to be shifted to the left compared with that of the SM channel; once again, those differences were in the wrong direction to help rationalize the voltage-dependent block by nisoldipine.

Given these observations, we had to conclude that the sensitivity difference to nisoldipine block of the two isoforms lies in some mechanism other than the inactivation gating of the channels. One possibility is the activation gating of the channels, which can directly or indirectly influence voltage-dependent drug actions (Kuo and Bean, 1994; Balser *et al.*, 1996), might differ in the two isoforms. We thus studied the current-voltage relations of the channels and deduced the activation curves from them (Fig. 4, A and B). The conductance-voltage curves, fit using $G = [1 + \exp(V_{½} - V)/k]^{-1}$, yielded parameters of $V_{½} = -16$ mV and $k = 8$ mV for the cardiac channel, and $V_{½} = -17$ mV and $k = 7$ mV for the SM one. The two channel isoforms are thus virtually identical in their activation properties.

Discussion

Our results demonstrate that isoform-specific sensitivity to DHP block is not caused by inactivation gating differences between the two channels. If anything, the cardiac (α1C-a) channels tended to inactivate at more negative potentials than the SM (α1C-b) channels, which would predict that nisoldipine would block the cardiac channel more potently. This prediction is the opposite of what we observed and of

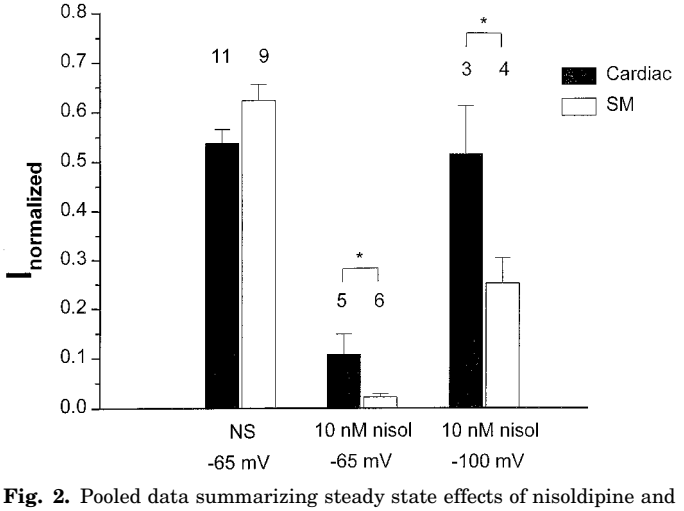

Fig. 2. Pooled data summarizing steady state effects of nisoldipine and V_h on cardiac and SM channels. I_{Ca} elicited from $V_h = -100$ mV to 0 mV in normal saline was used as the reference current (100%), and $I_{relative}$ was defined as the ratio of the remaining current to the reference current. Three pairs of bars represented relative currents at $V_h = -65$ mV, in the presence of 10 nM nisoldipine while V_h was still −65 mV, and when V_h was changed back to −100 mV while 10 nM nisoldipine was still present. *, statistically significant. Note that the SM channel was moderately less inactivated at −65 mV than the cardiac one, with a marginal p value of 0.056.

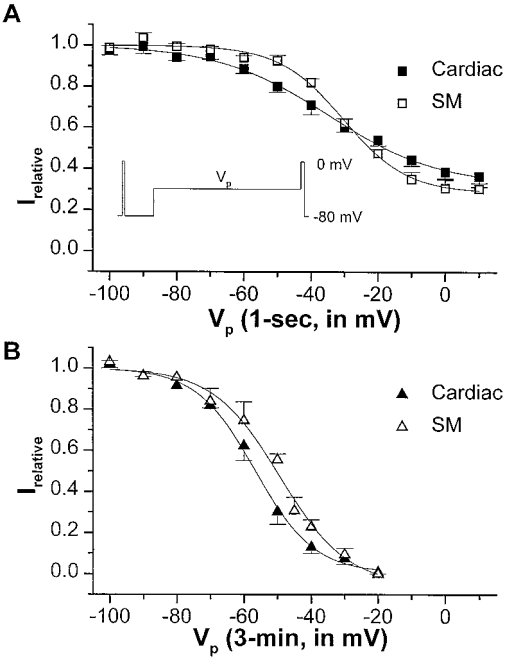

Fig. 3. Inactivation of the two isoforms of the channels. A, Fast inactivation of the cardiac (■, $n = 10$) and SM (□, $n = 10$) channels. The smooth curves represent Boltzmann fits. Paired t test of derived Boltzmann parameters ($V_{½}$ and k) from the original inactivation curves showed no difference between the two channel isoforms. *Inset,* double-pulse voltage protocol used in these experiments, which is composed of a 0-mV test pulse of 15 msec, a −80-mV reactivation pulse of 200 msec, a 1-sec inactivation prepulse to potential V_p, and a second 0-mV test pulse of 25 msec. B, Slow inactivation of the cardiac (▲) and SM (△) channels (see text). Pulses to V_p here lasted 3 min. Data were recorded from 12 cells expressing the cardiac channel and 14 cells expressing the SM channel. *Points*, averages of data from three to six cells. ANCOVA showed no significant differences between the two groups of data.

what has been described previously. We therefore have to propose that factors other than inactivation gating underlie the isoform-specific nisoldipine inhibition of L-type Ca^{2+} channels.

Our results indicate that some of the inactivation characteristics of the expressed channels are different from those reported previously in native cells. Fig. 3 shows that, for either type of the expressed channels, the inactivation was about 30% incomplete even after one second prepulses to 0 mV, and the slope of the cardiac channel inactivation was 17 mV. This is quite different from observations made in native cells, in which channels are generally completely inactivated under similar conditions, and the slope is ~7 mV (McDonald *et al.* 1994). There are reports, however, that when briefer prepulses (100–200 msec) were applied, 20% of channel activity remained (Lee *et al.,* 1985). Interestingly, a similar amount of remaining channel activity was observed in a *Xenopus laevis* oocyte expression system with prepulses as long as 5 sec (Parent *et al.,* 1995). Although there seem to be genuine (and unexplained) differences between native currents and those in heterologous expression systems, such differences do not affect our conclusions, which rely on internal comparisons within the HEK 293 expression system.

Welling *et al.* (1997) have identified transmembrane segment IS6 of the channels as responsible for the nisoldipine sensitivity differences by expressing carboxy-terminal truncated α1C-a or α1C-b subunits alone in HEK 293 cells. The α1C-a IS6 and α1C-b IS6 segments are alternatively spliced and selectively expressed in cardiac or SM cells. Although it has been suggested that this segment is involved in voltage-dependent inactivation (Zhang *et al.,* 1994; Parent *et al.,* 1995), our results unambiguously divorce any possible impact of inactivation from isoform-specific inhibition by DHPs. Our results also suggest that activation gating differences are not responsible for the isoform-specific inhibition. Thus, the isoform-specific inhibition by DHPs is not modulated by channel state or gating, although in general, the DHP inhibition of the channels is still heavily modulated by the membrane potential.

By exclusion, we conclude that the isoform-specific inhibition reflects an intrinsic DHP binding affinity difference between the two channel isoforms. The precise structural features of the DHP binding site remain to be determined. DHPs act on Ca^{2+} channels preferentially from the extracellular side of the cell (Kass and Arena, 1989). Photoaffinity and mutational analysis have suggested that the DHP binding domain is possibly composed of transmembrane segments IS6, IIIS6, IVS6, and the linker of IIIS5 and IIIS6 (Nakayama *et al.,* 1991; Striessnig *et al.,* 1991; Kalasz *et al.,* 1993; Schuster *et al.,* 1996), but not a cytosolic peptide directly after IVS6 as previously reported (Regulla *et al.,* 1991). It is not yet clear whether transmembrane segment IS6 or other parts of the channel are the critical features of the DHP-binding domain that confer voltage-dependent inhibition.

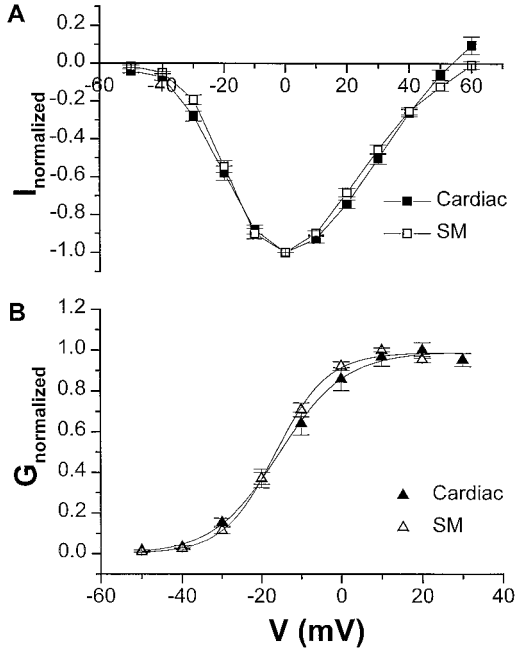

Fig. 4. Current-voltage relation and activation of the channels. A, Normalized current-voltage (*I-V*) relations of the cardiac (■) and the SM channel (□). There were no statistical differences between the curves. B, Normalized conductance-voltage (*G-V*) relations of the cardiac (▲) and the SM channel (△). The conductance was deduced from the data in A using $G = I/(V-V_{rev})$, where I is the current, G is the conductance, V is the membrane potential, and V_{rev} is the reversal potential. Smooth curves are Boltzmann fits. There are no significant differences between the two groups of data.

Acknowledgments

We thank Dr. Franz Hofmann (Institut für Pharmakologie und Toxikologie der Technischen Universitat, München, Germany) for the gift of subcloned α1C-a and α1C-b, Drs. Jeffrey Balser, Jean-Pierre Benitah, Jochen Rose, and Toshio Yamagishi for helpful discussions, and Maria Janecki for technical assistance.

References

Balser JR, Nuss HB, Orias DW, Johns DC, Marban E, Tomaselli GF, and Lawrence JH (1996) Local anesthetics as effectors of allosteric gating. Lidocaine effects on inactivation-deficient rat skeletal muscle Na^+ channels. *J Clin Invest* **98:**2874–2886.

Bean BP (1984) Nitrendipine block of cardiac calcium channels: high-affinity binding to the inactivated state. *Proc Natl Acad Sci USA* **81:**6388–6392.

Biel M, Ruth P, Bosse E, Hullin R, Stuhmer W, Flockerzi V, and Hofmann F (1990) Primary structure and functional expression of a high voltage activated calcium channel from rabbit lung. *FEBS Lett* **269:**409–412.

Catterall WA (1996) Molecular properties of sodium and calcium channels. *J Bioenerg Biomembr* **28:**219–230.

Ellis SB, Williams ME, Ways NR, Brenner R, Sharp AH, Leung AT, Campbell KP, McKenna E, Koch WJ, Hui A, Schwartz A, and Harpold MM (1988) Sequence and expression of mRNAs encoding the *alpha* 1 and *alpha* 2 subunits of a DHP-sensitive calcium channel. *Science (Washington DC)* **241:**1661–1664.

Graham FL and van der Eb AJ (1973) A new technique for the assay of infectivity of human adenovirus 5 DNA. *Virology* **52:**456–467.

Hamill OP, Marty A, Neher E, Sakmann B, and Sigworth FJ (1981) Improved patch-clamp techniques for high-resolution current recording from cells and cell-free membrane patches. *Pflueg Arch Eur J Physiol* **391:**85–100.

Hess P, Lansman JB, and Tsien RW (1984) Different modes of Ca channel gating behaviour favoured by dihydropyridine Ca agonists and antagonists. *Nature (Lond)* **311:**538–544.

Hille B (1977) Local anesthetics: hydrophilic and hydrophobic pathways for the drug-receptor reaction. *J Gen Physiol* **69:**497–515.

Hu H, Chiamvimonvat N, Yamagishi T, and Marban E (1997) Direct inhibition of expressed cardiac L-type Ca^{2+} channels by S-nitrosothiol nitric oxide donors. *Circ Res* **81:**742–752.

Kalasz H, Watanabe T, Yabana H, Itagaki K, Naito K, Nakayama H, Schwartz A, and Vaghy PL (1993) Identification of 1,4-dihydropyridine binding domains within the primary structure of the alpha 1 subunit of the skeletal muscle L-type calcium channel. *FEBS Lett* **331:**177–181.

Kass RS and Arena JP (1989) Influence of pH_o on calcium channel block by amlodipine, a charged dihydropyridine compound. Implications for location of the dihydropyridine receptor. *J Gen Physiol* **93:**1109–1127.

Kass RS and Krafte DS (1987) Negative surface charge density near heart calcium channels. Relevance to block by dihydropyridines. *J Gen Physiol* **89:**629–644.

Kass RS and Scheuer T (1982) Slow inactivation of calcium channels in the cardiac Purkinje fiber. *J Mol Cell Cardiol* **14:**615–618.

Kuo CC and Bean BP (1994) Na^+ channels must deactivate to recover from inactivation. *Neuron* **12:**819–829.

Lee KS, Marban E, and Tsien RW (1985) Inactivation of calcium channels in mam-

malian heart cells: joint dependence on membrane potential and intracellular calcium. *J Physiol (Lond)* **364:**395–411.
Marshall J, Molloy R, Moss GW, Howe JR, and Hughes TE (1995) The jellyfish green fluorescent protein: a new tool for studying ion channel expression and function. *Neuron* **14:**211–215.
McDonald TF, Pelzer S, Trautwein W, and Pelzer DJ (1994) Regulation and modulation of calcium channels in cardiac, skeletal, and smooth muscle cells. *Physiol Rev* **74:**365–507.
Mikami A, Imoto K, Tanabe T, Niidome T, Mori Y, Takeshima H, Narumiya S, and Numa S (1989) Primary structure and functional expression of the cardiac dihydropyridine-sensitive calcium channel. *Nature (Lond)* **340:**230–233.
Nakayama H, Taki M, Striessnig J, Glossmann H, Catterall WA, and Kanaoka Y (1991) Identification of 1,4-dihydropyridine binding regions within the alpha 1 subunit of skeletal muscle Ca^{2+} channels by photoaffinity labeling with diazipine. *Proc Natl Acad Sci USA* **88:**9203–9207.
Nelson MT, Laher I, and Worley J (1988) Membrane potential regulates dihydropyridine inhibition of single calcium channels and contraction of rabbit mesenteric artery. *Ann NY Acad Sci* **522:**47–50.
Parent L, Gopalakrishnan M, Lacerda AE, Wei X, and Perez-Reyes E (1995) Voltage-dependent inactivation in a cardiac-skeletal chimeric calcium channel. *FEBS Lett* **360:**144–150.
Perez-Reyes E, Castellano A, Kim HS, Bertrand P, Baggstrom E, Lacerda AE, Wei XY, and Birnbaumer L (1992) Cloning and expression of a cardiac/brain beta subunit of the L-type calcium channel. *J Biol Chem* **267:**1792–1797.
Perez-Reyes E and Schneider T (1995) Molecular biology of calcium channels. *Kidney Int* **48:**1111–1124.
Regulla S, Schneider T, Nastainczyk W, Meyer HE, and Hofmann F (1991) Identification of the site of interaction of the dihydropyridine channel blockers nitrendipine and azidopine with the calcium-channel *alpha* 1 subunit. *EMBO J* **10:**45–49.
Sanguinetti MC and Kass RS (1984) Voltage-dependent block of calcium channel current in the calf cardiac Purkinje fiber by dihydropyridine calcium channel antagonists. *Circ Res* **55:**336–348.
Schuster A, Lacinova L, Klugbauer N, Ito H, Birnbaumer L, and Hofmann F (1996) The IVS6 segment of the L-type calcium channel is critical for the action of dihydropyridines and phenylalkylamines. *EMBO J* **15:**2365–2370.
Schwartz A, Grupp IL, Grupp G, Williams JS, and Vaghy PL (1984) Effects of dihydropyridine calcium channel modulators in the heart: pharmacological and radioligand binding correlations. *Biochem Biophys Res Commun* **125:**387–394.
Striessnig J, Murphy BJ, and Catterall WA (1991) Dihydropyridine receptor of L-type Ca^{2+} channels: identification of binding domains for [^{3}H](+)-PN200–110 and [^{3}H]azidopine within the *alpha* 1 subunit. *Proc Natl Acad Sci USA* **88:**10769–10773.
Triggle DJ (1991) Calcium-channel drugs: structure-function relationships and selectivity of action. *J Cardiovasc Pharmacol* **18(**Suppl 10**):**S1–6.
Triggle DJ, Langs DA, and Janis RA (1989) Ca^{2+} channel ligands: structure-function relationships of the 1, 4-dihydropyridines. *Med Res Rev* **9:**123–180.
Vaghy PL, Striessnig J, Miwa K, Knaus HG, Itagaki K, McKenna E, Glossmann H, and Schwartz A (1987) Identification of a novel 1,4-dihydropyridine- and phenylalkylamine-binding polypeptide in calcium channel preparations. *J Biol Chem* **262:**14337–14342.
Welling A, Kwan YW, Bosse E, Flockerzi V, Hofmann F, and Kass RS (1993) Subunit-dependent modulation of recombinant L-type calcium channels. Molecular basis for dihydropyridine tissue selectivity. *Circ Res* **73:**974–980.
Welling A, Ludwig A, Zimmer S, Klugbauer N, Flockerzi V, and Hofmann F (1997) Alternatively spliced IS6 segments of the α_{1C} gene determine the tissue-specific dihydropyridine sensitivity of cardiac and vascular smooth muscle L-type Ca^{2+} channels. *Circ Res* **81:**526–532.
Zhang JF, Ellinor PT, Aldrich RW, and Tsien RW (1994) Molecular determinants of voltage-dependent inactivation in calcium channels. *Nature (Lond)* **372:**97–100.

Send reprint requests to: Eduardo Marban, M.D., Ph.D., 844 Ross Bldg., Johns Hopkins University, School of Medicine, Baltimore, MD 21205. E-mail: marban@welchlink.welch.jhu.edu